Mol Divers
DOI 10.1007/s11030-017-9733-z

SHORT COMMUNICATION

Synthesis and evaluation of novel HCV replication inhibitors

David C. McGowan[1] · Mourad D. Khamlichi[2] · Alex De Groot[1] · Frederik Pauwels[1] · Frédéric Delouvroy[1] · Kristof Van Emelen[1] · Kenneth Simmen[1] · Pierre Raboisson[1]

Received: 13 October 2016 / Accepted: 20 February 2017

Abstract Direct acting antiviral agents to cure hepatitis C virus (HCV) infection has emerged as the gold standard therapy. Along with protease inhibitors, nucleoside polymerase inhibitors and non-nucleoside polymerase inhibitors, the inhibition of NS5a has proved to be an effective way to treat HCV patients. Here we report on novel HCV NS5a inhibitors which were synthesized and evaluated in the HCV replicon assay. A series of inhibitors were formed by a cycloaddition reaction in parallel to establish new leads and explore the effects of unsymmetrical cap substitution. This led to the identification of several triazoles with picomolar potency in vitro against hepatitis C virus.

Graphical Abstract

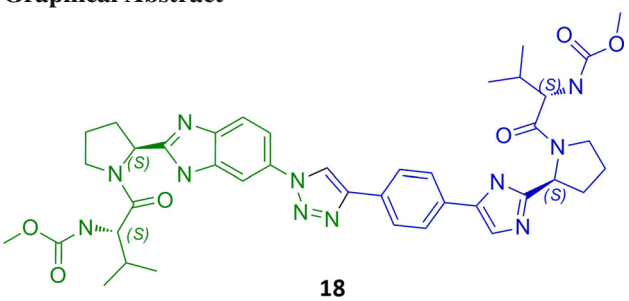

Electronic supplementary material The online version of this article (doi:10.1007/s11030-017-9733-z) contains supplementary material, which is available to authorized users.

✉ David C. McGowan
dmcgowan@its.jnj.com

[1] Janssen Infectious Diseases BVBA, Turnhoutseweg 30, 2340 Beerse, Belgium

[2] Villapharma Research, Parque Tecnológico de Fuente Álamo, Ctra. El Estrecho-Lobosillo, Km. 2,5- Av. Azul, 30320 Fuente Álamo de Murcia, Murcia, Spain

Keywords Hepatitis C · HCV NS5a · Replication inhibitor · Click chemistry

Introduction

Over 4 million people in the USA and 180 million worldwide are infected with hepatitis C virus (HCV) [1,2]. Chronic infection is the leading cause of cirrhosis and hepatocellular carcinoma globally [3]. Increased survival rates and improved clinical outcome are associated with sustained virologic response (SVR) [4,5] which has been shown to be achieved in clinic trials upon administration of approved direct acting antivirals (DAA) [6]. Clinical scenarios encompass the combination of medicaments to enhance the antiviral effect resulting in faster cure rates [7]. Among the therapeutic targets are the replication inhibitors effecting an RNA binding protein which also interacts with other HCV nonstructural proteins known as HCV NS5a [8,9]. Daclatasvir is a first-in-class HCV NS5a inhibitor that has shown a robust decline in viral HCV RNA in patients infected with HCV G1 [1,10,11]. This highly selective inhibitor has in vitro potency in the picomolar range. It is characterized by a central biphenyl scaffold further substituted at the 4,4′-positions by 2-(pyrrolidin-2-yl)-1*H*-imidazoles that are in turn acylated with amino acid derived moieties, termed caps. Modeling suggests that the biphenyl scaffold of Daclatasvir behaves as a spacer between the substituted heterocycles [12] and that there is evidence for an asymmetric binding to NS5a [13]. In this communication, we describe our synthetic effort toward novel inhibitors and their structure–activity relationship (Fig. 1).

Published online: 14 March 2017

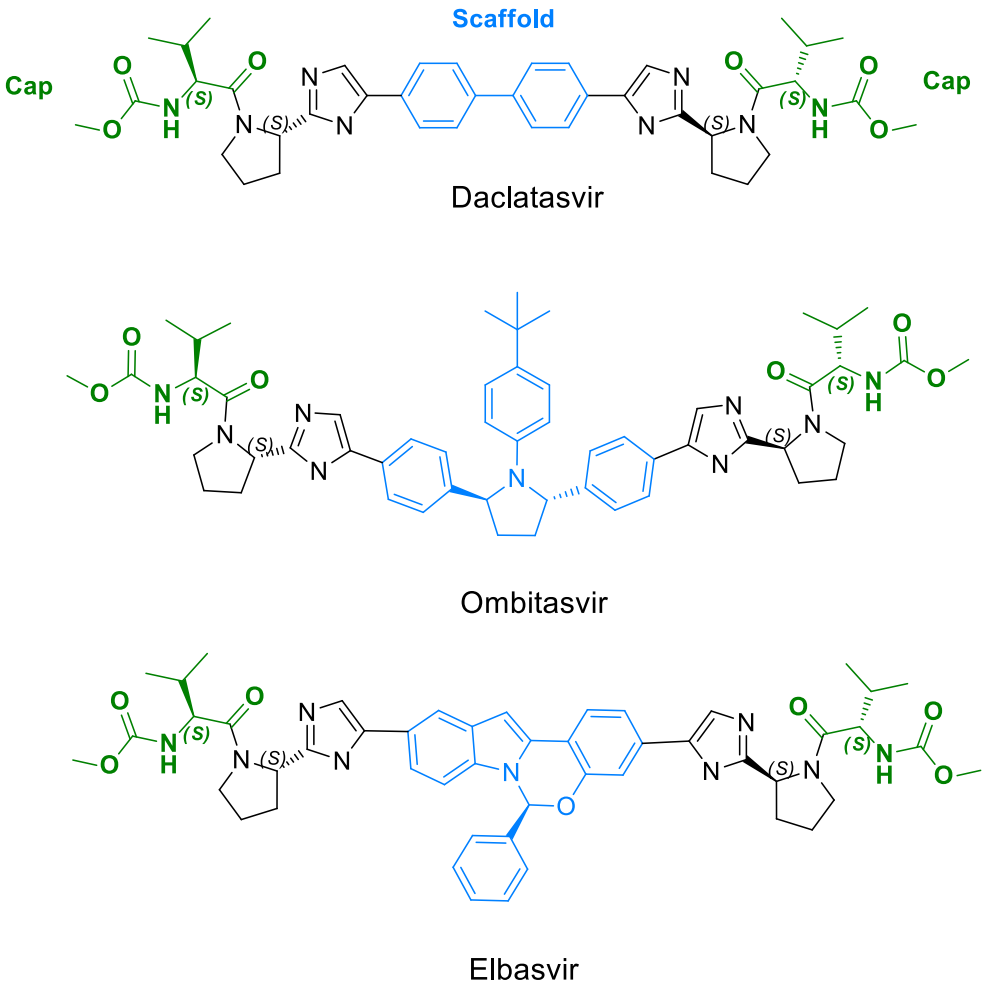

Fig. 1 Approved HCV NS5a inhibitors Daclatasvir [10,11], Ombitasvir [14] and Elbasvir [15]

Design strategy

The first NS5a inhibitors were discovered by screening in an in vitro assay for anti-HCV activity. The inhibitors later evolved into dimeric species [16] that offered exceptional potency and better genotype coverage and it has been recently described that unsymmetrical inhibitors could offer advantages in optimizing potency and pharmacokinetics [17]. Our goal was to discover an unsymmetrical series with high potency that could be assembled rapidly using combinatorial techniques.

In our design strategy, we proposed that it would be advantageous to design several monomeric unit permutations that could be easily fused together. We were interested to first modify the structural motifs to afford functionalized monomers with two different reactive handles. In principle, the monomers containing complimentary reactive handles could be combined together under mild conditions that would not affect the functional groups present. These modified fragments could then be linked to resemble a dimeric scaffold that would allow a combinatorial array of monomers with different caps on either side leading to a rapid assembly of unsymmetrical inhibitors (Fig. 2). Another advantage of the triazole central scaffold is that it does not contain additional chiral centers.

The Cu(I) catalyzed Huisgen azide–alkyne 1,3-dipolar cycloaddition was chosen because of facile access to the functional groups required for the reactive pairs, and the mild reaction conditions used to combine the alkyne and azide. Triazoles with symmetrical substitution have been previously described as inhibitors of HCV [18] but were not assembled via cycloaddition. Our effort was to explore the unsymmetrical 1,3-disubstituted triazole central core and to combine that with the combinatorial strategy for the end groups. To this point, three functionalized benzimidazole azides were prepared and cross-reacted with three terminal alkyne derivatives, as outlined in Scheme 1. The same three capping groups were used across each axis as shown in Table 1. The product combination via click chemistry under Sharpless conditions [19] therefore produced six products that were unsymmet-

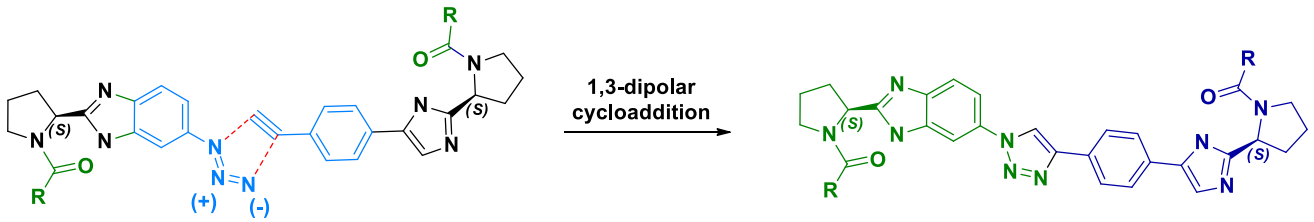

Fig. 2 Design strategy for novel HCV NS5a inhibitors

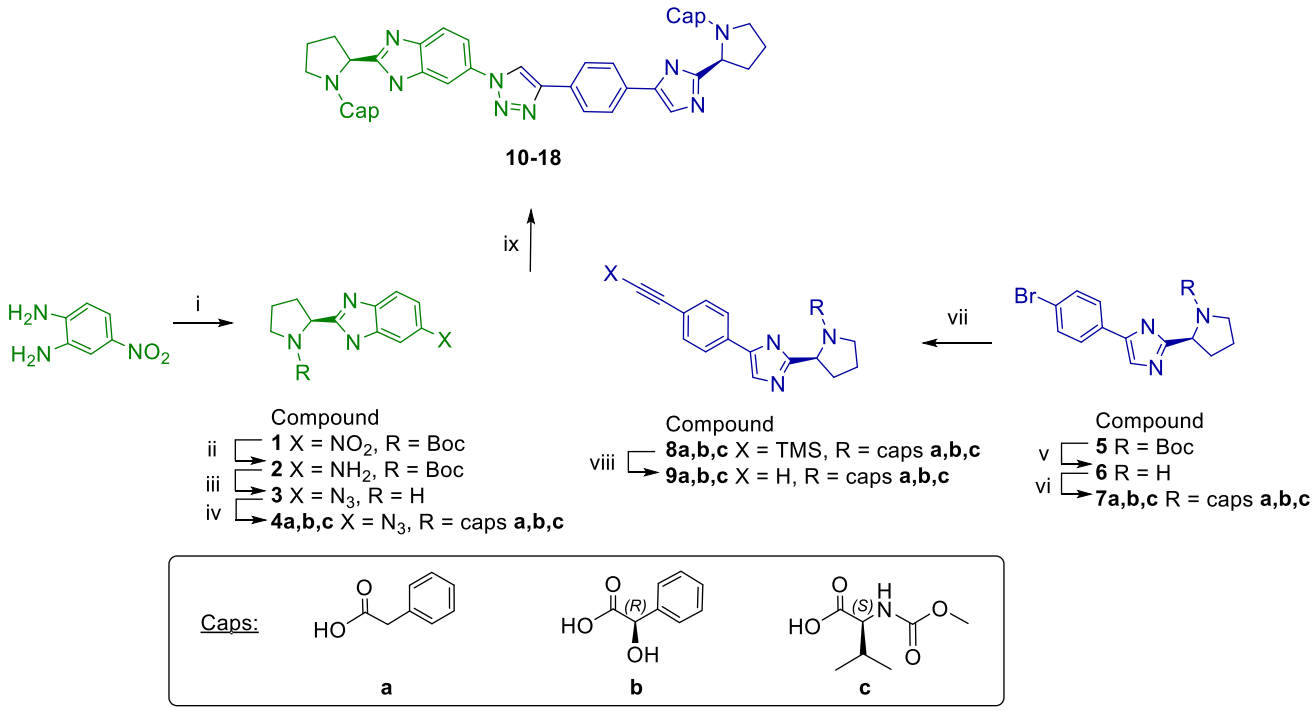

Scheme 1 Synthesis of the triazole series. Reagents and conditions: (i) Boc proline, CDI, pyridine/DMF 45 °C then 4-nitro-1,2-phenylenediamine, rt, 18h, HOAc, 100 °C, 1h; (ii) Pd/C, MeOH; (iii) $NaNO_2$, HCl, NaN_3, water; (iv) DIC, DIPEA, DMA, HOBt; (v) HCl; (vi) HATU, DIPEA, DMF; (vii) TMSCCH, $PdCl_2(PPh_3)_2$, CuI, Et_3N; (viii) K_2CO_3, CH_3OH; (ix) Na L-ascorbate, $CuSO_4$ $5H_2O$, *t*–BuOH/water(1/1), rt, 18h

rically capped and three that bore the same cap on either side.

Results and discussion

Formation of the aryl azides began with the reaction of Boc proline and carbonyldiimidazole (CDI), followed by the addition of 4-nitro-1,2-phenylenediamine to afford the protected benzimidazole **1** in 80% yield. Reduction of the nitro group via catalytic hydrogenation led to the aniline derivative **2**. Treatment of **2** with sodium nitrite in an aqueous HCl solution generated the arylazonium salt, which was reacted with NaN_3 to give the corresponding azide with concomitant Boc deprotection (**3**). The liberated amine **3** was condensed with three caps (**a**, **b** and **c**) using diisopropylcarbodiimide (DIC) or [(dimethylamino)-1*H*-1,2,3-triazolo-[4,5-*b*] pyridin-1-ylmethylene]-*N*-methylmethanaminium hexafluorophosphate *N*-oxide (HATU) coupling agents in dimethylacetamide (DMA) to yield the corresponding amides **4a**, **b**, **c** after flash chromatography in 70–90% yields.

The route toward the three alkyne derivatives started with arylbromide **5** [20], subsequent deprotection under acidic conditions (**6**) followed by installation of the capping groups (**a**, **b** and **c**) via HATU in DMF provided **7a**, **b**, **c**. Typical Sonogashira reaction conditions produced the TMS acetylene derivatives, followed by deprotection of the TMS group under basic conditions to give **9a**, **b**, **c**. Combination of the azides (**4a**, **4b**, **4c**) and the acetylenes (**9a**, **9b**, **9c**) via click chemistry under Sharpless conditions afforded triazoles **10**–**18** and their activities are shown in Table 1. The combination provided nine compounds with sub-nanomolar potency with the exception of **10** having a half-maximal effective concentration (EC_{50}) of 2.5 nM, bearing cap **a** on both sides.

Table 1 Activity of the combinatorial array of triazole products **10–18** in the HCV replicon assay

Compound EC_{50} /EC_{90} (nM)	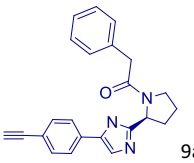 9a	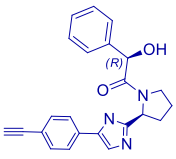 9b	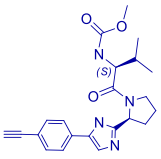 9c
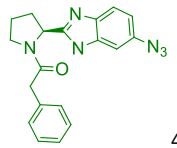 4a	**10** 2.5 / 5.8	**11** 0.04 / 0.20	**12** 0.17 / 0.65
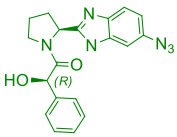 4b	**13** 0.2 / 0.7	**14** 0.5 / 1.5	**15** 0.6 / 2.5
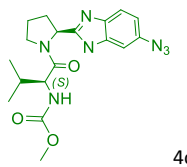 4c	**16** 0.1 / 0.6	**17** 0.02 / 0.07	**18** 0.02 / 0.07

The product structures are not shown but represented in the table (**10–18**). The 50% cytotoxic concentration (CCx_{50}) in Huh-7 and MT-4 cells was greater than the highest concentration tested (>0.1 μM). Daclatasvir displayed an EC_{50} of 0.01 nM (reported data 0.009 ± 0.004 nM [21]) in our assay

This series of novel HCV inhibitors explored the combinatorial approach where fragments were combined in a cycloaddition reaction in parallel. The combination of the valine carbamate cap **c**, on the benzimidazole side, with the (*R*)-mandelic amide cap **b**, on the acetylene side, identified **17** as a promising new lead. This finding was comparable with the combination of two valine carbamate caps (**18**). Conversely, swapping the caps on the same triazole, thus the valine carbamate cap **c**, on the alkyne side, with the (*R*)-mandelic amide cap **b**, on the benzimidazole fragment, led to a 30-fold less potent analog (**15**). This finding indicated that compounds **17** and **18** offered favorable disposition of the capping groups for optimal activity. This series warrants further exploration as potential anti-HCV agents

Experimental

Reagents and solvents were purchased from commercial sources and used without purification. Anhydrous solvents were obtained from Aldrich and used directly. Silica gel chromatography was generally performed with prepacked silica gel cartridges (from Biotage, Interchim, or Teledyne Isco). The purity of all compounds was determined by UPLC, conducted on Waters: Acquity® UPLC®-DAD and SQD systems, Waters HSS T3 column (1.8 μm, 2.1 × 100 mm, at 40° C). The mobile phase consisted of 10 mM CH_3COONH_4 in 95% H_2O + 5% CH_3CN (A) and CH_3CN (B). A gradient program was used as follows: From 100% A to 5% A in 2.10 min, to 0% A in 0.90 min, to 5% A in 0.5 min, at a flow rate of 0.8 mL/min. All compounds exhibited greater than 95% purity. ^1H and ^{13}C (APT) NMR experiments were performed at 27 °C on a Bruker Avance I—600 MHz. TMS or residual solvent shift of deuterated dimethyl sulfoxide (DMSO-d_6, ^1H: 2.5 ppm, ^{13}C: 39.51 ppm) was used as internal standard for calibration of spectra. The following standard abbreviations were used for signal multiplicities: singlet (s), doublet (d), triplet (t), multiplet (m) and broad signal (br. s.). Predominant forms are described. Minor signals of both tautomeric and rotameric forms were observed as well. High-resolution mass spectrometry was performed on a Waters Acquity® IClass UPLC®-DAD and Xevo G2-S QTOF. The samples were run on a Waters CSH C18 (1.7 μm, 2.1 × 50*mm*, at 50 °C) column, with a flow rate of 1 mL/min, using reverse phase chromatography with a gradient from 95% A to 5% A in 4.6 min, and held for 0.4min (A: 95% CH_3COONH_4 6.5 mM + 5% CH_3CN, B: CH_3CN). Melting points were measured with a differential scanning calorimeter (DSC) Mettler-Toledo DSC823e, applying a temperature gradient of 10 °C/minute, reaching a maximum temperature of 300 °C. Compounds **10** to **18** did not display a melting point (or temperature of glass transition).

Procedure for the synthesis of 2-((*S*)-pyrrolidin-2-yl)-6-(4-(4-(2-((*S*)-pyrrolidin-2-yl)-1*H*-imidazol-5-yl)phenyl)-1*H*-1,2,3-triazol-1-yl)-1*H*-benzo[*d*]imidazoles **10** to **18**. An alkyne (0.5 mmol), aryl azide (0.66 mmol), sodium L-ascorbate (1 mmol) and copper sulfate pentahydrate (0.1 mmol) were dissolved in *t*-butanol:water (1:1, 2 mL). The mixture was stirred overnight at room temperature. The solvent was removed under reduced pressure and the resulting crude material was purified via silica column chromatography using a CH_2Cl_2 to CH_2Cl_2 : CH_3OH (9:1) gradient.

*2-Phenyl-1-((S)-2-(5-(4-(1-(2-((S)-1-(2-phenylacetyl)pyrrolidin-2-yl)-1H-benzo[d]imidazol-6-yl)-1H-1,2,3-triazol-4-yl)phenyl)-1H-imidazol-2-yl)pyrrolidin-1-yl)ethanone (***10***)* Yellow solid, 6% yield.^{1}H NMR (DMSO-d_6) δ ppm 1.92–2.18 (m, 7 H), 2.26–2.32 (m, 1 H), 3.55–3.62 (m, 1 H), 3.63–3.69 (m, 1 H), 3.71–3.82 (m, 5 H), 3.88 (t, J = 7.7 Hz, 1 H), 5.09 (dd, J = 7.7, 2.2 Hz, 1 H), 5.22 (dd, J = 8.5, 2.7 Hz, 1 H), 7.19–7.33 (m, 10 H), 7.54 (d, J = 1.9 Hz, 1 H), 7.66–7.68 (m, 1 H), 7.75–7.79 (m, 1 H), 7.86 (br d, J = 8.3 Hz, 2 H), 7.89–7.97 (m, 2 H), 8.08 (s, 1 H), 9.20–9.26 (m, 1 H), 11.83 (br s, 1 H). ^{13}C NMR (DMSO-d_6)δ 24.1, 24.2, 31.2, 31.3, 40.7, 40.9, 46.9, 47.1, 54.5, 55.0, 110.2, 112.1, 112.5, 114.8, 119.6, 124.6, 125.4, 126.3, 127.7, 128.0, 128.1, 129.4, 129.5, 131.3, 133.9, 134.8, 135.3, 135.5, 139.0, 143.2, 147.2, 149.6, 158.5, 169.2, 169.4. ESI-HRMS (TOF) m/z: 702.3301 (Calcd. for $C_{42}H_{39}N_9O_2$[M+H]$^+$: 702.3305).

*(R)-2-Hydroxy-2-phenyl-1-((S)-2-(5-(4-(1-(2-((S)-1-(2-phenylacetyl)pyrrolidin-2-yl)-1H-benzo[d]imidazol-6-yl)-1H-1,2,3-triazol-4-yl)phenyl)-1H-imidazol-2-yl)pyrrolidin-1-yl)ethanone (***11***)* Yellow solid, 28% yield. ^{1}H NMR (DMSO-d_6)δ ppm 1.80–1.86 (m, 1 H), 1.96–2.19 (m, 6 H), 2.26–2.32 (m, 1 H), 3.08–3.14 (m, 1 H), 3.63–3.69 (m, 1 H), 3.73 (d, J = 15.8 Hz, 1 H), 3.79 (d, J = 15.8 Hz, 1 H), 3.81–3.85 (m, 1 H), 3.85–3.91 (m, 1 H), 5.08 (br dd, J = 7.1, 3.0 Hz, 1 H), 5.22 (br dd, J = 8.4, 2.7 Hz, 1 H), 5.27 (d, J = 6.4 Hz, 1 H), 7.15–7.20 (m, 1 H), 7.20–7.24 (m, 1 H), 7.25–7.28 (m, 2 H), 7.28–7.32 (m, 2 H), 7.36–7.40 (m, 2 H), 7.40–7.43 (m, 2 H), 7.65–7.71 (m, 1 H), 7.72–7.79 (m, 2 H), 7.86 (br d, J = 7.8 Hz, 2 H), 7.95 (br d, J = 7.8 Hz, 2 H), 8.03–8.11 (m, 1 H), 9.22–9.28 (m, 1 H), 11.97 (br s, 1 H), 12.43–12.66 (m, 1 H). ^{13}C NMR (DMSO-d_6)δ 24.0, 24.3, 31.0, 31.3, 40.8, 46.2, 47.2, 55.0, 55.1, 72.2, 110.3, 112.2, 114.9, 119.7, 124.7, 125.5, 126.4, 127.6, 128.0, 128.2, 128.5, 129.6, 131.4, 134.1, 135.4, 139.7, 143.4, 147.3, 149.6, 158.5, 169.5, 170.8. ESI-HRMS (TOF) m/z: 718.3255 (Calcd. for $C_{42}H_{39}N_9O_3$[M+H]$^+$: 718.3254).

*Methyl ((S)-3-methyl-1-oxo-1-((S)-2-(5-(4-(1-(2-((S)-1-(2-phenylacetyl)pyrrolidin-2-yl)-1H-benzo[d]imidazol-6-yl)-1H-1,2,3-triazol-4-yl)phenyl)-1H-imidazol-2-yl)pyrrolidin-1-yl)butan-2-yl)carbamate (***12***)* Yellow solid, 14% yield. ^{1}H NMR (DMSO-d_6)δ ppm 0.85 (br d, J = 6.6 Hz, 3 H), 0.90 (br d, J = 6.9 Hz, 3 H), 1.91–2.04 (m, 4 H), 2.07–2.17 (m, 4 H), 2.24–2.30 (m, 1 H), 3.53 (s, 3 H), 3.62–3.67 (m, 1 H), 3.69–3.82 (m, 4 H), 3.84 - 3.88 (m, 1 H), 4.07 (br t, J = 8.3 Hz, 1 H), 5.05–5.09 (m, 1 H), 5.21 (dd, J = 8.4, 2.3 Hz, 1 H), 7.20 (t, J = 7.4 Hz, 1 H), 7.24 (d, J = 7.6 Hz, 2 H), 7.26–7.31 (m, 2 H), 7.53 (s, 1 H), 7.65 (d, J = 8.5 Hz, 1 H), 7.73–7.76 (m, 1 H), 7.82 (br d, J = 7.9 Hz, 2 H), 7.88–7.92 (m, 2 H), 8.05–8.08 (m, 1 H), 9.18–9.23 (m, 1 H), 11.79 (br s, 1 H), 12.43–12.62 (m, 1 H). ^{13}C NMR (DMSO-d_6) δ 18.6, 19.0, 24.3, 29.9, 31.0, 31.3, 31.4, 40.9, 46.9, 47.2, 51.5, 54.4, 55.0, 55.1, 58.1, 110.3, 112.2, 112.7, 114.9, 124.6, 125.5, 126.4, 127.8, 128.2, 129.6, 131.4, 134.0, 135.0, 135.5, 138.9, 143.4, 147.3, 149.4, 156.9, 158.6, 169.5, 170.5. ESI-HRMS (TOF) m/z: 741.3617 (Calcd. for $C_{41}H_{44}N_{10}O_4$[M+H]$^+$: 741.3625).

*(R)-2-Hydroxy-2-phenyl-1-((S)-2-(6-(4-(4-(2-((S)-1-(2-phenylacetyl)pyrrolidin-2-yl)-1H-imidazol-5-yl)phenyl)-1H-1,2,3-triazol-1-yl)-1H-benzo[d]imidazol-2-yl)pyrrolidin-1-yl)ethanone (***13***)* White solid, 6% yield. ^{1}H NMR (DMSO-d_6)δ ppm 1.84–2.19 (m, 8 H), 3.13–3.19 (m, 1 H), 3.57–3.62 (m, 1 H), 3.72 (s, 2 H), 3.78–3.83 (m, 1 H), 3.88–3.92 (m, 1 H), 5.09 (dd, J = 7.9, 1.9 Hz, 1 H), 5.21 (dd, J = 7.9, 2.6 Hz, 1 H), 5.32 (d, J = 6.0 Hz, 1 H), 5.47 (br d, J = 6.0 Hz, 1 H), 7.20–7.24 (m, 2 H), 7.27–7.35 (m, 4 H), 7.37–7.41 (m, 2 H), 7.41–7.44 (m, 2 H), 7.55 (d, J = 1.9 Hz, 1 H), 7.68–7.71 (m, 1 H), 7.75–7.80 (m, 1 H), 7.87 (d, J = 8.3 Hz, 2 H), 7.89–7.96 (m, 2 H), 8.07 - 8.11 (m, 1 H), 9.25 (br d, J = 5.7 Hz, 1 H), 11.82 (br s, 1 H), 12.51–12.72 (m, 1 H).^{13}C NMR (DMSO-d_6) δ 24.1, 24.1, 30.9, 31.2, 40.9, 46.4, 46.9, 54.5, 55.5, 72.1, 110.3, 112.1, 112.5, 114.9, 119.6, 124.6, 125.4, 126.2, 127.6, 127.8, 128.0, 128.1, 128.4, 129.4, 131.3, 133.9, 134.8, 135.5, 139.0, 139.6, 143.3, 147.3, 149.6, 158.3, 169.2, 170.9. ESI-HRMS (TOF) m/z: 718.3247 (Calcd. for $C_{42}H_{39}N_9O_3$[M+H]$^+$: 718.3254).

*(R)-2-Hydroxy-1-((S)-2-(5-(4-(1-(2-((S)-1-((R)-2-hydroxy-2-phenylacetyl)pyrrolidin-2-yl)-1H-benzo[d]imidazol-6-yl)-1H-1,2,3-triazol-4-yl)phenyl)-1H-imidazol-2-yl)pyrrolidin-1-yl)-2-phenylethanone (***14***)* Yellow solid, 9% yield. ^{1}H NMR (DMSO-d_6) δ ppm 1.80–1.93 (m, 2 H), 1.95–2.19 (m, 6 H), 3.08–3.14 (m, 1 H), 3.14–3.19 (m, 1 H), 3.80–3.85 (m, 1 H), 3.87–3.92 (m, 1 H), 5.08 (dd, J = 7.3, 2.6 Hz, 1 H), 5.21 (dd, J = 7.9, 2.6 Hz, 1 H), 5.27 (d, J = 6.3 Hz, 1 H), 5.32 (d, J = 6.3 Hz, 1 H), 5.45 (br d, J = 6.5 Hz, 1 H), 5.47 (d, J = 6.6 Hz, 1 H), 7.31–7.35 (m, 2 H), 7.37–7.44 (m, 8 H), 7.51–7.56 (m, 1 H), 7.67–7.72 (m, 1 H), 7.74–7.80 (m, 1 H), 7.86 (br d, J = 7.3 Hz, 2 H), 7.95 (br d, J = 7.9 Hz, 2 H), 8.06–8.12 (m, 1 H), 9.25 (br s, 1 H), 11.96 (br s, 1 H), 12.57–12.76 (m, 1 H). ^{13}C NMR (DMSO-d_6) δ 24.0, 24.2, 31.0, 46.3, 46.5, 55.1, 55.6, 72.1, 72.2, 110.4, 112.2, 115.0, 119.4, 119.8, 124.7, 125.6, 127.6, 127.7, 127.9, 128.0, 128.5, 128.5, 131.4, 134.0, 139.7, 139.7, 143.4, 147.3, 149.6, 158.4, 170.8, 171.0. ESI-HRMS (TOF) m/z: 734.3205 (Calcd. for $C_{42}H_{39}N_9O_4$[M+H]$^+$: 734.3203).

Methyl ((S)-1-((S)-2-(5-(4-(1-(2-((S)-1-((R)-2-hydroxy-2-phenylacetyl)pyrrolidin-2-yl)-1H-benzo[d]imidazol-6-yl)-1H-

*1,2,3-triazol-4-yl)phenyl)-1H-imidazol-2-yl)pyrrolidin-1-yl) -3-methyl-1-oxobutan-2-yl)carbamate (***15***)* Yellow solid, 15% yield. ^{1}H NMR (DMSO-d_6)δ ppm 0.86 (br d, J = 6.6 Hz, 3 H), 0.92 (br d, J = 6.3 Hz, 3 H), 1.85–1.90 (m, 1 H), 1.93–2.05 (m, 4 H), 2.09–2.19 (m, 4 H), 3.13–3.19 (m, 1 H), 3.55 (s, 3 H), 3.79–3.84 (m, 2 H), 3.87–3.92 (m, 1 H), 4.08 (br t, J = 8.3 Hz, 1 H), 5.09 (dd, J = 7.2, 3.5 Hz, 1 H), 5.21 (dd, J = 7.9, 2.6 Hz, 1 H), 5.32 (d, J = 6.2 Hz, 1 H), 5.47 (br d, J = 6.5 Hz, 1 H), 7.31–7.35 (m, 1 H), 7.39 (t, J = 7.8 Hz, 2 H), 7.41–7.44 (m, 2 H), 7.53–7.56 (m, 1 H), 7.69 (br d, J = 8.5 Hz, 1 H), 7.74–7.79 (m, 1 H), 7.81–7.87 (m, 2 H), 7.89–7.96 (m, 2 H), 8.09 (s, 1 H), 9.20–9.28 (m, 1 H), 11.81 (br s, 1 H), 12.57–12.73 (m, 1 H). ^{13}C NMR (DMSO-d_6)δ 18.6, 19.0, 24.1, 24.3, 29.9, 31.0, 46.5, 46.9, 51.5, 54.3, 55.6, 58.1, 72.1, 110.4, 112.2, 112.7, 115.0, 119.7, 124.6, 125.5, 127.7, 128.0, 128.5, 131.4, 134.0, 135.0, 139.7, 143.3, 147.4, 149.4, 156.9, 158.4, 170.5, 171.0. ESI-HRMS (TOF) m/z: 757.3571 (Calcd. for $C_{41}H_{44}N_{10}O_5[M+H]^+$: 757.3574).

*Methyl ((S)-3-methyl-1-oxo-1-((S)-2-(6-(4-(4-(2-((S)-1-(2-ph enylacetyl)pyrrolidin-2-yl)-1H-imidazol-5-yl)phenyl)-1H-1, 2,3-triazol-1-yl)-1H-benzo[d]imidazol-2-yl)pyrrolidin-1-yl) butan-2-yl)carbamate (***16***)* Yellow solid, 7% yield.^{1}H NMR (DMSO-d_6)δ ppm 0.82–0.89 (m, 6 H), 1.91–2.00 (m, 2 H), 2.00–2.16 (m, 4 H), 2.20–2.30 (m, 3 H), 3.55 (s, 3 H), 3.57–3.62 (m, 1 H), 3.72 (s, 2 H), 3.78–3.90 (m, 3 H), 4.10 (br t, J = 8.4 Hz, 1 H), 5.07–5.10 (m, 1 H), 5.22 (br s, 1 H), 7.20–7.24 (m, 1 H), 7.25–7.33 (m, 4 H), 7.46–7.58 (m, 1 H), 7.66 (br d, J = 8.2 Hz, 1 H), 7.76 (br d, J = 8.5 Hz, 1 H), 7.82–7.88 (m, 2 H), 7.92–7.96 (m, 2 H), 8.06 (s, 1 H), 9.22–9.27 (m, 1 H), 11.82 (br s, 1 H), 12.49–12.59 (m, 1 H). ^{13}C NMR (DMSO-d_6)δ 18.3, 19.0, 24.1, 24.5, 29.6, 31.0, 31.3, 40.9, 47.0, 47.0, 51.5, 54.4, 54.8, 57.9, 110.2, 112.1, 114.9, 119.6, 124.6, 125.5, 128.0, 128.1, 129.4, 131.2, 133.9, 135.5, 143.0, 147.2, 149.5, 156.9, 158.3, 169.3, 170.6. ESI-HRMS (TOF) m/z: 741.3629 (Calcd. for $C_{41}H_{44}N_{10}O_4$[M+H]$^+$: 741.3625).

*Methyl ((S)-1-((S)-2-(6-(4-(4-(2-((S)-1-((R)-2-hydroxy-2-ph enylacetyl)pyrrolidin-2-yl)-1H-imidazol-5-yl)phenyl)-1H-1, 2,3-triazol-1-yl)-1H-benzo[d]imidazol-2-yl)pyrrolidin-1-yl) -3-methyl-1-oxobutan-2-yl)carbamate (***17***)* Yellow solid, 23% yield. ^{1}H NMR (DMSO-d_6) δ ppm 0.84 (br d, J = 6.4 Hz, 3 H), 0.88 (br d, J = 6.4 Hz, 3 H), 1.80–1.86 (m, 1 H), 1.92–2.11 (m, 5 H), 2.18–2.31 (m, 3 H), 3.08–3.14 (m, 1 H), 3.55 (s, 3 H), 3.79–3.91 (m, 3 H), 4.10 (t, J = 8.3 Hz, 1 H), 5.06–5.11 (m, 1 H), 5.20 - 5.24 (m, 1 H), 5.27 (br s, 1 H), 5.41–5.49 (m, 1 H), 7.31–7.35 (m, 1 H), 7.39 (t, J = 7.3 Hz, 2 H), 7.41–7.43 (m, 2 H), 7.56 (br s, 1 H), 7.65–7.73 (m, 1 H), 7.71–7.80 (m, 1 H), 7.86 (br d, J = 8.3 Hz, 2 H), 7.95 (br d, J = 7.9 Hz, 2 H), 8.02–8.10 (m, 1 H), 9.26 (br s, 1 H), 11.98 (br s, 1 H), 12.51–12.65 (m, 1 H). ^{13}C NMR (DMSO-d_6) δ 18.4, 19.0, 23.9, 24.5, 29.6, 30.9, 46.2, 47.0, 51.5, 54.8, 55.0, 57.9, 72.1, 110.3, 112.1, 114.8, 119.6, 124.6, 125.5, 127.5, 127.8, 128.4, 131.3, 134.0, 139.7, 143.1, 147.2, 149.5, 156.8, 158.2, 170.6, 170.7. ESI-HRMS (TOF) m/z: 757.3578 (Calcd. for $C_{41}H_{44}N_{10}O_5$[M+H]$^+$: 757.3574).

*Methyl ((S)-1-((S)-2-(6-(4-(4-(2-((S)-1-((S)-2-((methoxycar bonyl)amino)-3-methylbutanoyl)pyrrolidin-2-yl)-1H-imida zol-5-yl)phenyl)-1H-1,2,3-triazol-1-yl)-1H-benzo[d]imidaz ol-2-yl)pyrrolidin-1-yl)-3-methyl-1-oxobutan-2-yl)carbama te (***18***)* Yellow solid, 27% yield. ^{1}H NMR (DMSO-d_6) δ ppm 0.82–0.94 (m, 12 H), 1.92–2.32 (m, 10 H), 3.53–3.57 (m, 6 H), 3.79–3.92 (m, 4 H), 4.08 (br t, J = 8.4 Hz, 1 H), 4.10 (br t, J = 8.4 Hz, 1 H), 5.09 (dd, J = 7.2, 3.4 Hz, 1 H), 5.20–5.26 (m, 1 H), 7.29 (d, J = 8.5 Hz, 1 H), 7.32 (d, J = 8.5 Hz, 1 H), 7.54 (br s, 1 H), 7.66 (br d, J = 8.4 Hz, 1 H), 7.76 (br dd, J = 8.3, 1.5 Hz, 1 H), 7.80–7.86 (m, 2 H), 7.92 (br s, 2 H), 8.06 (s, 1 H), 9.22–9.27 (m, 1 H), 11.81 (br s, 1 H), 12.52–12.60 (m, 1 H). ^{13}C NMR (DMSO-d_6)δ 18.4, 18.5, 19.0, 19.0, 24.3, 24.5, 29.7, 29.8, 30.9, 30.9, 46.8, 47.0, 51.4, 51.4, 54.2, 54.8, 57.9, 58.0, 110.3, 112.1, 112.7, 114.8, 119.6, 124.5, 125.4, 127.8, 131.3, 134.0, 134.9, 138.8, 143.2, 147.2, 149.3, 156.8, 156.8, 158.3, 170.4, 170.6. ESI-HRMS (TOF) m/z: 780.3946 (Calcd. for $C_{40}H_{49}N_{11}O_6$[M+H]$^+$: 780.3945).

Biological assay

The in vitro antiviral activity against HCV was tested in a cellular HCV replicon system as previously described by Lohmann et al. [22], with the further modifications described by Krieger et al. [23]. The assay utilized the stably transfected cell line Huh-7 luc/neo (Huh-Luc). This cell line harbors an RNA encoding a bicistronic expression construct comprising the wild-type NS3-NS5B regions of HCV type 1b translated from an Internal Ribosome Entry Site (IRES) from encephalomyocarditis virus (EMCV), preceded by a reporter portion (FfL-luciferase) and a selectable marker portion (neoR, neomycine phosphotransferase). The construct is flanked by 5′ and 3′ NTRs (non-translated regions) from HCV type 1b. Continued culture of the replicon cells in the presence of G418 (neoR) is dependent on the replication of the HCV RNA. The stably transfected replicon cells that express HCV RNA, which replicates autonomously and to high levels, encoding inter alia luciferase, were used for screening the antiviral compounds. The replicon cells were plated in 384-well plates in the presence of the test and control compounds which were added in various concentrations. Following an incubation of three days, HCV replication was measured by assaying luciferase activity (using standard luciferase assay substrates and reagents and a PerkinElmer ViewLuxTM ultraHTS microplate imager). Replicon cells in the control cultures have high luciferase expression in the absence of any inhibitor. The inhibitory activity of the compound on luciferase activity was monitored on the Huh-Luc cells, enabling a dose–response curve for each test com-

pound. EC_{50} values were then calculated, which represent the amount of compound required to decrease the level of detected luciferase activity by 50%, or more specifically, to reduce the ability of the genetically linked HCV replicon RNA to replicate. CC_{50} values were evaluated in Huh7.5 parental cells by the MTS assay (CellTiter 96® AQueous One Solution Cell Proliferation kit, Promega). Cells treated with DMSO, without compound, served as control.

Acknowledgements The authors would like to thank the analytical teams at Janssen Infectious Diseases and Villapharma Research, including Alberto Fontana for HRMS data.

References

1. Lok AS, Gardiner DF, Lawitz E, Martorell C, Everson G, Ghalib R, Reindollar R, Rustgi V, McPhee F, Wind-Rotolo M, Persson A, Zhu K, Dimitrova DI, Eley T, Guo T, Grasela DM, Pasquinelli C (2013) Preliminary study of two antiviral agents for hepatitis C genotype 1. N Engl J Med 366:216–224. doi:10.1056/NEJMoa1104430
2. Messina JP, Humphreys I, Flaxman A, Brown A, Cooke GS, Pybus OG, Barnes E (2015) Global distribution and prevalence of hepatitis C virus genotypes. Hepatology 61:77–87. doi:10.1002/hep.27259
3. Perz JF, Armstrong GL, Farrington LA, Hutin YJ, Bell BP (2006) The contributions of hepatitis B virus and hepatitis C virus infections to cirrhosis and primary liver cancer worldwide. J Hepatol 45:529–538. doi:10.1016/j.jhep.2006.05.013
4. Morgan TR, Ghany MG, Kim HY, Snow KK, Shiffman ML, De Santo JL, Lee WM, Di Bisceglie AM, Bonkovsky HL, Dienstag JL, Morishima C, Lindsay KL, Lok AS (2010) Outcome of sustained virological responders with histologically advanced chronic hepatitis C. Hepatology 52:833–844. doi:10.1002/hep.23744
5. European Association for the Study of the Liver (2016) EASL Recommendations on Treatment of Hepatitis C 2016. J Hepatol 66:153–194. doi:10.1016/j.jhep.2016.09.001
6. Sherman KE, Flamm SL, Afdhal NH, Nelson DR, Sulkowski MS, Everson GT, Fried MW, Adler M, Reesink HW, Martin M, Sankoh AJ, Adda N, Kauffman RS, George S, Wright CI, Poordad F (2011) Response-guided telaprevir combination treatment for hepatitis C virus infection. N Engl J Med 365:1014–1024. doi:10.1056/NEJMoa1014463
7. Woodcock J, Griffin JD, Behrman RE (2011) Development of novel combination therapies. N Engl J Med 364:985–987. doi:10.1056/NEJMp1101548
8. Penin F, Brass V, Appel N, Ramboarina S, Montserret R, Ficheux D, Blum HE, Bartenschlager R, Moradpour D (2004) Structure and function of the membrane anchor domain of hepatitis C virus nonstructural protein 5A. J Biol Chem 279:40835–40843. doi:10.1074/jbc.M404761200
9. McGivern DR, Masaki T, Williford S, Ingravallo P, Feng Z, Lahser F, Asante-Appiah E, Neddermann P, De Francesco R, Howe AY, Lemo SM (2014) Kinetic analyses reveal potent and early blockade of hepatitis C virus assembly by NS5A inhibitors. Gastroenterology 147:453–462. doi:10.1053/j.gastro.2014.04.021
10. Belema M, Lopez OD, Bender JA, Romine JL, Laurent DR, Langley DR, Lemm JA, O'Boyle DR II, Sun JH, Wang C, Fridell RA, Meanwell NA (2014) Discovery and development of hepatitis C virus NS5A replication complex inhibitors. J Med Chem 57:1643–1672. doi:10.1021/jm401793m
11. Belema M, Nguyen V, Bachand C, Deon D, Goodrich J, James C, Lavoie R, Lopez O, Martel A, Romine J (2014) Hepatitis C virus NS5A replication complex inhibitors: the discovery of daclatasvir. J Med Chem 57:2013–2032. doi:10.1021/jm401836p
12. Cordek DG, Bechtel JT, Maynard AT, Kazmierski WM, Cameron CE (2011) Targeting the NS5a protein of HCV: an emerging option. Drug Future 36:691–711. doi:10.1358/dof.2011.036.09.1641618
13. Nettles JH, Stanton RA, Broyde J, Amblard F, Zhang H, Zhou L, Shi J, McBrayer TR, Whitaker T, Coats SJ, Kohler JJ, Schinazi RF (2014) Asymmetric binding to NS5A by Daclatasvir (BMS-790052) and analogs suggests two novel modes of HCV inhibition. J Med Chem 57:10031–10043. doi:10.1021/jm501291c
14. DeGoey DA, Randolph JT, Liu D, Pratt J, Hutchins C, Donner P, Krueger AC, Matulenko M, Patel S, Motter CE, Nelson L, Keddy R, Tufano M, Caspi DD, Krishnan P, Mistry N, Koev G, Reisch TJ, Mondal R, Pilot-Matias T, Gao Y, Beno DA, Maring CJ, Molla A, Dumas E, Campbell A, Williams L, Collins C, Wagner R, Kati WM (2014) Discovery of ABT-267, a pan-genotypic inhibitor of HCV NS5A. J Med Chem 57:2047–2057. doi:10.1021/jm401398x
15. Coburn CA, Meinke PT, Chang W, Fandozzi CA, Graham DJ, Hu B, Huang Q, Kargman S, Kozlowski J, Liu R, McCauley JA, Nomeir AA, Soll RM, Vacca JP, Wang D, Wu H, Zhong B, Olsen DB, Ludmerer SW (2013) Discovery of MK-8742: an HCV NS5A inhibitor with broad genotype activity. ChemMedChem 8:1930–1940. doi:10.1002/cmdc.201300343
16. Lemm JA, O'Boyle D, Liu M, Nower PT, Colonno R, Deshpande M, Snyder LB, Martin SW, St Laurent DR, Serrano-Wu MH, Romine JL, Meanwell NA, Gao M (2010) Identification of hepatitis C virus NS5A inhibitors. J Virol 84:482–491. doi:10.1128/JVI.01360-09
17. Link JO, Taylor JG, Xu L, Mitchell M, Guo H, Liu H, Kato D, Kirschberg T, Sun J, Squires N, Parrish J, Keller T, Yang ZY, Yang C, Matles M, Wang Y, Wang K, Cheng G, Tian Y, Mogalian E, Mondou E, Cornpropst M, Perry J, Desai MC (2014) Discovery of Ledipasvir (GS-5885): a potent, once-daily oral NS5A inhibitor for the treatment of hepatitis C virus infection. J Med Chem 57:2033–2046. doi:10.1021/jm401499g
18. Shi J, Zhou L, Amblard F, Bobeck DR, Zhang H, Liu P, Bondada L, McBrayer TR, Tharnish PM, Whitaker T, Coats SJ, Schinazi RF (2012) Synthesis and biological evaluation of new potent and selective HCV NS5A inhibitors. Bioorg Med Chem Lett 22:3488–3491. doi:10.1016/j.bmcl.2012.03.089
19. Rostovtsev VV, Green LG, Fokin VV, Sharpless KB (2002) A stepwise Huisgen cycloaddition process: copper(I)-catalyzed regioselective "ligation" of azides and terminal alkynes. Angew Chem Int Ed 41:2596–2599. doi:10.1002/1521-3773(20020715)41
20. Kazmierski WM, Maynard A, Duan M, Baskaran S, Botyanszki J, Crosby R, Dickerson S, Tallant M, Grimes R, Hamatake R, Leivers M, Roberts C, Walker J (2014) Novel spiroketal pyrrolidine GSK2336805 potently inhibits key hepatitis C virus genotype 1b mutants: from lead to clinical compound. J Med Chem 57:2058–2073. doi:10.1021/jm4013104
21. Gao M, Nettles RE, Belema M, Snyder LB, Nguyen VN, Fridell RA, Serrano-Wu MH, Langley DR, Sun J-H, O'Boyle DR, Lemm JA, Wang C, Knipe JO, Chien C, Colonno RJ, Grasela DM, Meanwell NA, Hamann LD (2010) Chemical genetics strategy identifies an HCV NS5A inhibitor with a potent clinical effect. Nature 465:96–100. doi:10.1038/nature08960
22. Lohmann V, Körner F, Koch J, Herian U, Theilmann L, Bartenschlager R (1999) Replication of subgenomic hepatitis C virus RNAs in a hepatoma cell line. Science 285:110–113. doi:10.1126/science.285.5424.110
23. Krieger N, Lohmann V, Bartenschlager R (2001) Enhancement of hepatitis C virus RNA replication by cell culture-adaptive mutations. J Virol 75:4614–4624. doi:10.1128/JVI.75.10.4614-4624.200